$\sigma\pi^*$ Orthogonal Intramolecular Charge-Transfer (OICT) Excited States and Photoreaction Mechanism of Trifluoromethyl-Substituted Phenyldisilanes[1]

Mitsuo Kira,*,†,‡ Takashi Miyazawa,‡ Hisashi Sugiyama,† Munehiro Yamaguchi,† and Hideki Sakurai*,†

Contribution from the Department of Chemistry, Faculty of Science, Tohoku University, Aoba-ku, Sendai 980, Japan, and Photodynamics Research Center, The Institute of Physical and Chemical Research (RIKEN), Koeji, Nagamachi, Aoba-ku, Sendai 982, Japan

Received October 14, 1992

Abstract: Photophysical and photochemical properties of phenyldisilanes having a trifluoromethyl substituent on a benzene ring as one of the most suitable substituents for stabilization of the OICT ($\sigma\pi^*$ orthogonal intramolecular charge transfer) state were investigated in detail. The OICT mechanism for CT fluorescence in nonpolar solvents was supported by the remarkable dependence of absorption and fluorescence spectra of trifluoromethyl-substituted phenyldisilanes on the dihedral angle between benzene pπ orbital and the SiSi σ bond. The detailed analysis of the steady-state photolysis of (*p*-trifluoromethylphenyl)pentamethyldisilane (**1b**) in the presence of alcohols revealed the nature of the excited states responsible for the photoreactions; the [1,3]-silyl migration occurs from an aromatic $\pi\pi^*$ (LE) state, while the direct alcoholysis of the aryldisilane takes place from the OICT state.

Introduction

In recent years, there has been considerable effort devoted to studies of the unique electronic properties and photoreactivity of aryl- and vinyldisilanes.[2] In 1964, Sakurai and Kumada,[3] Gilman et al.,[4] and Hague and Prince[5] reported independently that aryl- and vinyl-substituted polysilanes showed appreciable red shift of the absorption maxima of the corresponding monosilanes. Although these reports constitute the first recognition of the conjugation between a silicon–silicon bond and a phenyl or a vinyl π system, these conjugating properties were first rationalized in terms of "d–π^*" interaction in the excited state. Later, the σ–π conjugation between a Si–Si σ orbital and a pπ orbital has been taken to be the origin of the unique electronic properties, on the basis of the results of the charge-transfer (CT)[6,7] and photoelectron spectroscopic studies[8] of phenyldisilanes, and the remarkable stereoelectronic effects[9] on the absorption spectra;[10] in this model, the high-lying HOMO of an aryl–SiSi system is represented mainly by the linear combination of the σ(SiSi) orbital with the HOMO of the aromatic π system, while the population of the σ(SiSi) orbital in the HOMO of the aryl–SiSi system depends on the HOMO level of the aromatic π system.[6b]

Recently unusual dual fluorescence phenomena of aryldisilanes have been reported by Shizuka et al.[11] Thus, in addition to a regular emission band from an aromatic $\pi\pi^*$ (LE, locally excited) state a broad band at longer wavelength has been observed, which has been assigned to the emission from a CT excited state (2pπ^*, 3dπ(Si) state). However, their model, in which the disilanyl group and the aromatic π system are assumed to work as an electron acceptor and an electron donor, respectively, was incompatible with the well-confirmed electron-donating character of the silicon–silicon σ bond. On the basis of a study of substituent and solvent effects on the dual fluorescence of phenylpentamethyldisilane, we have proposed the orthogonal intramolecular charge-transfer (OICT) mechanism as another model,[12] involving a $\sigma\pi^*$ state as the CT excited state, in which the disilanyl group and the aromatic π system are taken as an electron donor and an electron acceptor, respectively. The conformational demands in the OICT mechanism[12] are also significantly different from those in the Shizuka's model[11] (vide infra).

Much attention has been focused on the photoreactions of aryldisilanes, since they generate interesting reactive silicon species such as silylenes, silenes, and silyl radicals, as has been shown by the chemical trapping experiments.[2,3,14-18] The photolysis of phenyldisilanes in the presence of alcohols gives rise to four types

† Tohoku University.
‡ RIKEN.

(1) Chemistry of Organosilicon Compounds. 300.
(2) (a) Sakurai, H. *J. Organomet. Chem.* **1980**, *200*, 261. (b) Ishikawa, M.; Kumada, M. *Adv. Organomet. Chem.* **1981**, *19*, 51.
(3) Sakurai, H.; Kumada, M. *Bull. Chem. Soc. Jpn.* **1964**, *37*, 1894.
(4) Gilman, H.; Atwell, W. H.; Schwebke, G. L. *J. Organomet. Chem.* **1964**, *2*, 369.
(5) Hague, D. N.; Prince, R. H. *Chem. Ind. (London)* **1964**, 1492.
(6) (a) Sakurai, H.; Kira, M. *J. Am. Chem. Soc.* **1974**, *96*, 791. (b) Sakurai, H.; Kira, M. *J. Am. Chem. Soc.* **1975**, *97*, 4879.
(7) (a) Bock, H.; Alt, H. *J. Am. Chem. Soc.* **1970**, *92*, 1569. (b) Pitt, C. G.; Carey, R. N.; Toren, E. C., Jr. *J. Am. Chem. Soc.* **1972**, *94*, 3806.
(8) Pitt, C. G.; Bock, H. *J. Chem. Soc., Chem. Commun.* **1972**, 28.
(9) Sakurai, H.; Tasaka, S.; Kira, M. *J. Am. Chem. Soc.* **1972**, *94*, 9285.
(10) For other studies on the electronic structure of phenyldisilanes, see: (a) Sakurai, H.; Yamamori, H.; Kumada, M. *Bull. Chem. Soc. Jpn.* **1965**, *38*, 2024. (b) Sakurai, H.; Tominaga, K.; Kumada, M. *Bull. Chem. Soc. Jpn.* **1966**, *39*, 1279. (c) Sakurai, H.; Yamamori, H.; Kumada, M. *J. Chem. Soc., Chem. Commun.* **1968**, 198. (d) Sakurai, H.; Ichinose, M.; Kira, M.; Traylor, T. G. *Chem. Lett.* **1984**, 1383. (e) Gilman, H.; Atwell, W. H. *J. Organomet. Chem.* **1965**, *4*, 176–178. (f) Gilman, H.; Atwell, W. H.; Sen, P. K.; Smith, C. L. *J. Organomet. Chem.* **1965**, *4*, 163. (g) Gilman, H.; Morris, P. J. *J. Organomet. Chem.* **1966**, *6*, 102. (h) Pitt, C. G. *J. Am. Chem. Soc.* **1969**, *91*, 6613–6622. (i) Pitt, C. G. *J. Chem. Soc., Chem. Commun.* **1971**, 816. (j) Ramsey, B. G. *Electronic Transitions in Organometalloids*; Academic Press: New York, 1969.
(11) (a) Shizuka, H.; Obuchi, H.; Ishikawa, M.; Kumada, M. *J. Chem. Soc., Chem. Commun.* **1981**, 405. (b) Shizuka, H.; Sato, Y.; Ishikawa, M.; Kumada, M. *J. Chem. Soc., Chem. Commun.* **1982**, 439. (c) Shizuka, H.; Sato, Y.; Ueki, Y.; Ishikawa, M.; Kumada, M. *J. Chem. Soc., Faraday Trans. 1* **1984**, *80*, 341. (d) Shizuka, H.; Obuchi, H.; Ishikawa, M.; Kumada, M. *J. Chem. Soc., Faraday Trans. 1* **1984**, *80*, 383. (e) Shizuka, H.; Okazaki, K.; Tanaka, M.; Ishikawa, M.; Sumitani, M.; Yoshihara, K. *Chem. Phys. Lett.* **1985**, *113*, 89. (f) Hiratsuka, H.; Mori, Y.; Ishikawa, M.; Okazaki, K.; Shizuka, H. *J. Chem. Soc., Faraday Trans. 2* **1985**, *81*, 1665.
(12) OICT is a conceptually similar term to TICT (twisted intramolecular charge transfer)[13] which is originally proposed for the dual fluorescence of (dimethylamino)benzonitrile. Similar to TICT ($n\pi^*$) and suddenly polarized ($\pi\pi^*$) states, OICT state is stabilized by taking a conformation in which donor and acceptor orbitals are mutually perpendicular. To reach such conformation in ($n\pi^*$) and ($\pi\pi^*$) states, molecular frames should also be twisted, but in ($\sigma\pi^*$) system, molecular frames should be coplanar to get orthogonal orbital arrangement. To avoid possible confusion, we have proposed the OICT as a general term. (a) Sakurai, H.; Sugiyama, H.; Kira, M. *J. Phys. Chem.* **1990**, *94*, 1837. (b) Sakurai, H. In *Silicon Chemistry*; Corey, J. Y., Corey, E. Y., Gaspar, P. P., Eds.; Ellis Horwood, Chichester: 1988; Chapter 16.

0002-7863/93/1515-3116$04.00/0

of reaction as outlined in Scheme I: (i) formation of a silaethene (I) via elimination of a hydrosilane (type 1),[14] (ii) formation of a silatriene (II) via 1,3-silyl migration (type 2),[15] (iii) elimination of a silylene (III) (type 3),[15a,16b] and (iv) nucleophilic cleavage of an SiSi bond in the excited state (type 4).[12b,17a]

The detailed mechanism of photoreactions would require not only determination of the real intermediates generated by the primary photoreactions but also the assignment of the excited electronic states responsible to the primary processes. In this context, the mechanistic aspects of the photolysis of aryldisilanes are still fragmentary and a matter of controversy. In a previous paper[16a] we have proposed that a primary photochemical process of phenyldisilanes in nonpolar solvents may be homolytic cleavage of the silicon–silicon σ bond in the excited state. Prominent transient species observed in nanosecond flash photolysis of aryldisilanes have been characterized to be silatriene intermediates II.[11e,19] On the basis of the results of steady-state and time-resolved fluorescence emission studies, II has been proposed to arise from direct [1,3]-silyl migration in a $^1(2p\pi^*,3d\pi)$ CT state of phenyldisilanes by Shizuka et al.[11e]

In this paper, we report a detailed study of the photochemical and photophysical properties of phenyldisilanes having a trifluoromethyl substituent on a benzene ring as one of the most suitable substituents for stabilization of the OICT state. The OICT mechanism for the CT fluorescence in nonpolar solvents was supported by the remarkable dependence of the absorption and fluorescence spectra of the phenyldisilanes on the dihedral angle between benzene $p\pi$ orbital and the SiSi σ bond. The detailed analysis of the steady-state photolysis of (*p*-trifluoromethylphenyl)pentamethyldisilane in the presence of alcohols revealed the nature of the excited states responsible for the photoreactions; the [1,3]-silyl migration occurs from LE, while the direct alcoholysis of the aryldisilane takes place mainly from the OICT state.

Results and Discussion

Stereoelectronic Effects on the Absorption Spectra of Trifluoromethyl-Substituted Disilanes. We have previously reported remarkable stereoelectronic effects on the absorption spectra of phenyldisilanes.[10] Thus, phenylpentamethyldisilane (**1a**), (2-methylphenyl)pentamethyldisilane (**4a**), and 1-(trimethylsilyl)-1-methyl-2,3-benzo-1-silacyclopentane (**2a**) showed intense absorption (^1L_a) maxima at around 230 nm, while no characteristic ^1L_a band was observed for 1,1,2,2-tetramethyl-3,4-benzo-1,2-disilacyclopentane (**3a**). Concerning the dihedral angle between

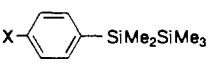

1a, X = H; 1b, X = CF_3

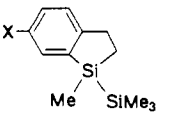

2a, X = H; 2b, X = CF_3

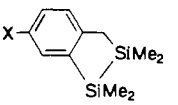

3a, X = H; 3b, X = CF_3

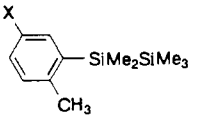

4a, X = H; 4b, X = CF_3

a Si–Si bond and a benzene ring plane, **2a** is fixed in the approximately perpendicular conformation A, while **3a** is in nearly in-plane conformation B. The longer wavelength ^1L_a absorption observed in **1a** and **4a** as well as **2a** is indicative of not only the significant σ–π conjugation in these aryldisilanes but also the conformation A as the preferred ground-state conformation of **1a** and **4a**; the conformational preference derived has also been supported by a recent free-jet laser spectroscopic study.[20] In terms of the configuration interaction method,[22] it would be described that the ^1L_a state of **1a** includes a major contribution from a ($\sigma\pi^*$) intramolecular CT configuration in which the σ-(SiSi) and the π system act as a donor and an acceptor, respectively, in addition to minor contributions from the local $^1B_{1u}$ configuration of benzene and a ($\sigma\sigma^*$) configuration of disilane.

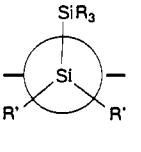

A

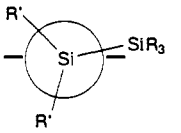

B

Similar conformational dependence was observed for a series of trifluoromethyl-substituted phenyldisilanes. As shown in Figure 1, (2-methyl-5-trifluoromethylphenyl)pentamethyldisilane (**4b**) showed the ^1L_a absorption maxima at 240 nm, which is ca. 10 nm longer than that of **4a**, suggesting the strengthening of the ($\sigma\pi^*$) intramolecular CT nature in the ^1L_a excited state by the electron-withdrawing trifluoromethyl substituent.

Although the forbidden ^1L_b absorption band was mostly hidden by the intense and broad ^1L_a band and therefore appeared as a weak shoulder, the ^1L_b state would be the lowest singlet excited state for the trifluoromethyl-substituted phenyldisilanes at the Franck–Condon conformation (conformation A).

Stereoelectronic Fluorescence Spectra in Nonpolar Solvents. On the basis of a study of the emission spectra of various aryldisilanes, we have proposed[12] ($\sigma\pi^*$) orthogonal charge-transfer (OICT) mechanism for the unique dual fluorescence of aryldisilanes, whereas Shizuka et al. have assigned the long wavelength fluorescence band to the $^1(2p\pi^*,3d\pi)$ intramolecular charge-transfer state. Although the basis of our model has been discussed thoroughly in the previous paper, here is given the additional evidence for the ($\sigma\pi^*$) nature of the CT state. Thus, in accord with the ($\sigma\pi^*$) CT model, *p*-trifluoromethyl- (**1b**) and (*p*-cyanophenyl)pentamethyldisilane having a strong electron-

(13) For a recent review, see: Rettig, W. *Angew. Chem., Int. Ed. Engl.* **1986**, *25*, 971.

(14) Boudjouk, P.; Roberts, J. R.; Golino, C. M.; Sommer, L. H. *J. Am. Chem. Soc.* **1972**, *94*, 7926–7927.

(15) (a) Ishikawa, M. *Pure Appl. Chem.* **1978**, *50*, 11. (b) Ishikawa, M.; Fuchikami, T.; Sugaya, T.; Kumada, M. *J. Am. Chem. Soc.* **1975**, *97*, 5923. (c) Ishikawa, M.; Fuchikami, T.; Kumada, M. *J. Organomet. Chem.* **1976**, *118*, 139. (d) Ishikawa, M.; Fuchikami, T.; Kumada, M. *J. Organomet. Chem.* **1976**, *118*, 155. (e) Ishikawa, M.; Fuchikami, T.; Kumada, M. *Tetrahedron Lett.* **1976**, 1299. (f) Ishikawa, M.; Fuchikami, T.; Kumada, M. *J. Organomet. Chem.* **1977**, *133*, 19. (g) Ishikawa, M.; Fuchikami, T.; Kumada, M. *J. Organomet. Chem.* **1978**, *162*, 223. (h) Ishikawa, M.; Oda, M.; Miyoshi, N.; Fabry, L.; Kumada, M.; Yamabe, T.; Akagi, K.; Fukui, K. *J. Am. Chem. Soc.* **1979**, *101*, 4612. (i) Ishikawa, M.; Oda, M.; Nishimura, K.; Kumada, M. *Bull. Chem. Soc. Jpn.* **1983**, *56*, 2795. (j) Ohshita, J.; Ohsaki, H.; Ishikawa, M.; Tachibana, A.; Kurosaki, Y.; Yamabe, T.; Minato, A. *Organometallics* **1991**, *10*, 880. (k) Takaki, K.; Sakamoto, H.; Nishimura, Y.; Sugihara, Y.; Ishikawa, M. *Organometallics* **1991**, *10*, 888. (l) Ohshita, J.; Ohsaki, H.; Ishikawa, M.; Tachibana, A.; Kurosaki, Y.; Yamabe, T.; Tsukihara, T.; Takahashi, K.; Kiso, Y. *Organometallics* **1991**, *10*, 2685. (m) Ohshita, J.; Ohsaki, H.; Ishikawa, M. *Organometallics* **1991**, *10*, 2695. (n) Ishikawa, M.; Nishimura, Y.; Sakamoto, H. *Organometallics* **1991**, *10*, 2701.

(16) (a) Sakurai, H.; Nakadaira, Y.; Kira, M.; Sugiyama, H.; Yoshida, K.; Takiguchi, T. *J. Organomet. Chem.* **1980**, *184*, C36. (b) Kira, M.; Sakamoto, K.; Sakurai, H. *J. Am. Chem. Soc.* **1983**, *105*, 7469. (c) Sakurai, H.; Sakamoto, K.; Kira, M. *Chem. Lett.* **1984**, 1213.

(17) (a) Okinoshima, H.; Weber, W. P. *J. Organomet. Chem.* **1978**, *149*, 279. (b) Hu, S.-S.; Weber, W. P. *J. Organomet. Chem.* **1989**, *369*, 155.

(18) Coleman, B.; Jones, M., Jr. *Rev. Chem. Intermediates* **1981**, *4*, 297.

(19) Sluggett, G. W.; Leigh, W. J. *J. Am. Chem. Soc.* **1992**, *114*, 1195.

(20) The dihedral angles at the MM2 optimized geometries of **1a**, **2a**, and **3a** were 80–90°, 80.3°, and 15.7°, respectively.[21]

(21) Kira, M.; Miyazawa, T.; Mikami, N.; Sakurai, H. *Organometallics* **1991**, *10*, 3794.

(22) (a) Longuet-Higgins, H. C.; Murrell, J. N. *Proc. Phys. Soc. (London)* **1955**, *A68*, 601. (b) Murrell, J. N. *Proc. Phys. Soc. (London)* **1955**, *A68*, 969. (c) Nagakura, S.; Tanaka, J. *J. Chem. Phys.* **1954**, *22*, 236. (d) Nagakura, S. *Pure and Appl. Chem.* **1963**, *7*, 79. (e) Nagakura, S.; Kojima, N.; Maruyama, Y. *J. Mol. Spectrosc.* **1964**, *13*, 174. (f) Kimura, K.; Nagakura, S. *Mol. Phys.* **1965**, *8*, 117. (g) Nagakura, S.; Kimura, K. *J. Chem. Soc. Jpn.* **1965**, *86*, 1.

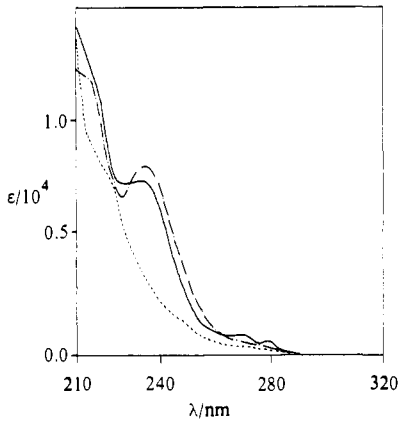

Figure 1. Absorption spectra of **2b** (—), **3b** (– –), and **4b** (– · –) in hexane at room temperature.

Table 1. Fluorescence Band Maxima and the Lifetimes for Several *p*-Substituted Phenylpentamethyldisilanes (p-$XC_6H_4SiMe_2SiMe_3$) in Pentane

	λ_{max}, nm			
X	LE	CT	$(\tau/ns)^a$	σ^b
Me_2N	325	*c*	(3.2)	–0.83
MeO	302	*c*	(2.6)	–0.27
Me	297	*c*	*d*	–0.17
H	296	340	$(<1)^{e,f}$	0
CF_3	*c*	366	$(<1)^f$	0.54
CN	*c*	379	$(<1)^f$	0.66

[a] Fluorescence lifetimes were measured under the irradiation of 250-nm light with a nanosecond time-resolved fluorescence spectrometer. See also Experimental Section. [b] Hammett's σ constant taken from ref 23. [c] Not observed. [d] Not measured. [e] Two-component decays with the lifetimes of 30 and 150 ps were observed by picosecond laser flash photolysis.[11e] [f] Too short to be measured.

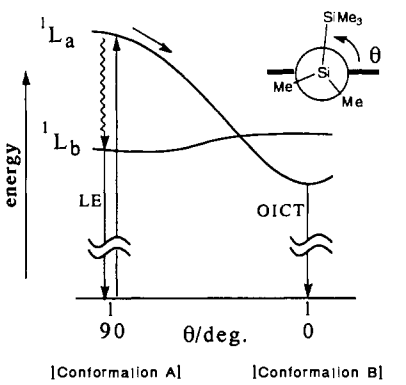

Figure 2. Schematic potential surfaces for OICT mechanism in **1b**.

withdrawing substituent on benzene showed the significant long wavelength shift of the CT fluorescence band in a hydrocarbon solvent than that of the parent phenylpentamethyldisilane, as shown in Table I. The very short fluorescence lifetimes (<1 ns) observed for these phenyldisilanes having a strong electron-withdrawing substituent are also characteristic for CT emission; whereas p-Me_2N- and p-MeO-substituted phenyldisilanes showed emission bands at rather longer wavelength region, the bands are assigned to LE emission, on the basis of the relatively long lifetimes as well as the intense and sharp band pattern.

In the OICT mechanism, it is expected that the OICT state of a phenyldisilane is formed by excitation at the perpendicular conformation A followed by internal rotation about the C(aryl)–Si bond. The excited-state potential surfaces along the reaction coordinate toward the OICT state in aryldisilanes will be represented as shown schematically in Figure 2. In this concern, we have previously compared the fluorescence spectra of **1a** and **4a** with those of the model compounds, **2a** and **3a**,[12] where the

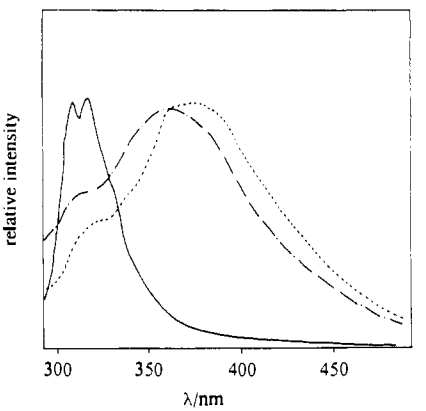

Figure 3. Fluorescence spectra of **2b** (—), **3b** (– –), and **4b** (– · –) in hexane at room temperature.

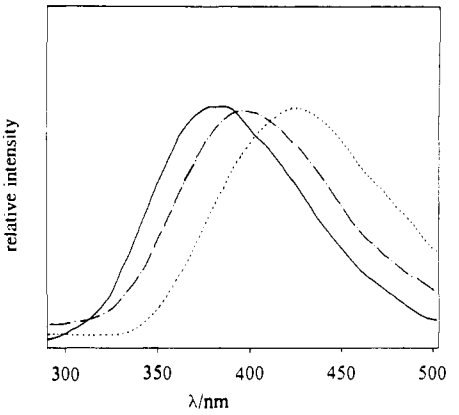

Figure 4. Fluorescence spectra of **2b** (—), **3b** (– –), and **4b** (– · –) in dichloromethane at room temperature.

SiSi bond was rigidly held in the perpendicular and planar conformation, respectively. However, in a nonpolar solvent, these phenyldisilanes did not show the CT emission with enough intensity to allow the discussion about the validity of the OICT mechanism. Remarkable stereoelectronic effects on the fluorescence spectra were observed for trifluoromethyl-substituted phenyldisilanes, **2b**, **3b**, and **4b**, in hexane (Figure 3); **2b** showed intense and sharp LE emission but lacked the CT emission, while a typical broad CT emission band accompanied by a weak LE emission band was observed for both **3b** and **4b**. Thus, **2b** having the geometry which is suitable for strong σ–π conjugation but prohibits the formation of OICT state showed the intense UV absorption maxima at around 240 nm but no CT emission. On the other hand, **3b** having the geometry in which the σ–π overlap is less effective but the CT excited state is stabilized well showed the typical CT emission, while no intense CT absorption was observed because of the overalp forbiddenness. The fact that the absorption spectrum of **4b** resembles that of **2b**, while the emission spectrum of **4b** was similar to that of **3b**, is in good accord with the OICT mechanism for the CT emission of **4b**; the absorption occurs at the preferred conformation A and then the OICT state would be formed at the conformation B via a dynamic relaxation with internal rotation about the C(aryl)–Si bond.

Contrary to the OICT mechanism, **2b** showed the CT emission in dichloromethane, which is more polar than hexane (Figure 4); the CT emission maxima appeared at a little shorter wavelength than those for **3b** and **4b**. As pointed out in a previous paper,[12a] these results may suggest that in polar solvents, the stabilization of the CT excited states is achieved by a mechanism not yet specified, instead of the OICT mechanism.

Solvent Effects on Fluorescence Spectra. The dependence of the band maxima and the quantum yields for the CT emission of **1b** on the solvent polarity was investigated in dichloromethane–hexane solvent mixtures. As shown in Table II, both the

Table 11. Solvent Effects on the Fluorescence Band Maxima and the Quantum Yields of **1b** in Dichloromethane–Hexane Mixtures[a]

$[CH_2Cl_2]$,[b] M	λ_{max}, nm	Φ_{rel}[c]	$[CH_2Cl_2]$,[b] M	λ_{max}, nm	Φ_{rel}[c]
0.0	367	1.0	4.65	389	7.30
1.48	381	2.62	6.58	395	9.01
1.87	381	3.36	9.09	404	13.0
2.22	383	3.36	12.3	412	15.2
3.09	390	4.93			

[a] Concentration of **1b** in the mixed solvents and the temperature was fixed to 6.14×10^{-5} M and 22.5 ± 0.5 °C, respectively. [b] Molar concentration of dichloromethane in hexane. [c] Fluorescence quantum yield relative to that in pure hexane under irradiation of 254-nm light. The absolute quantum yield in pure hexane was determined to be 3.3×10^{-3} by comparing the fluorescence intensity to that of naphthalene in hexane (0.19).[25]

wavelength of the band maximum and the quantum yield for the CT emission increased with increasing concentration of dichloromethane in hexane, i.e., with increasing the solvent polarity, as expected by the CT nature of the emission. The kinetics of the dual fluorescence phenomena would be represented by a diagram shown schematically in Figure 5, where k_f and k_f' are the fluorescence rate constants for LE and CT states, respectively, k_D and k_D' are the inherent rate constants for unimolecular deactivation of LE and CT, respectively. We assume here that k_C, the rate constant for the formation of CT from LE, is represented by a linear function of the concentration of a polar-solvent (S), i.e., dichloromethane in the present case (eq 1). Although the CT state may not be formed via the LE state but may be directly formed from higher excited states at the Franck–Condon geometry, eq 1 may embody properly the increase of efficiency of the CT formation with increasing the solvent polarity.[24] If the model in Figure 5 is valid, the CT fluorescence quantum yield ϕ_f' should be represented by eq 3. The quantum yield of the CT fluorescence in the absence of S ($\phi_f'^0$) divided by the quantum yield in the presence of S (ϕ_f') is represented by eq 4. By assuming $k_C^0 < k_C[S]$ at higher concentrations of the polar cosolvent, a plot of $\phi_f'^0/\phi_f'$ vs $1/[S]$ is predicted to give a straight line, where the intercept should be equal to the quantum yield of the formation of CT state in the nonpolar solvent. The prediction was actually satisfied by the relationship shown in Figure 6 (slope, 0.445; intercept, 0.051; correlation coefficient, 0.991).

$$k_C = k_C^0 + k_C'[S] \tag{1}$$

$$\Phi_C = \frac{k_C^0 + k_C'[S]}{k_D + k_f + k_C^0 + k_C'[S]} \tag{2}$$

$$\Phi_f' = \Phi_C \times \frac{k_f'}{k_D' + k_f'} \tag{3}$$

$$\frac{\Phi_f'^0}{\Phi_f'} = \frac{k_C^0}{k_D + k_f + k_C^0}\left(1 + \frac{k_D + k_f}{k_C^0 + k_C'[S]}\right) \tag{4}$$

In contrast to rather reasonable solvent effects on the CT fluorescence in dichloromethane and dichloromethane–hexane mixtures, **1b** did not show the intense emission in acetonitrile and ethanol. The CT fluorescence band maxima in ethanol–hexane mixtures shifted red, but the quantum yields decreased with increasing the concentration of ethanol in hexane. These results suggest that the fluorescence would be quenched by nucleophilic solvents like ethanol and acetonitrile.[26] Since the quenching may be strongly related to the solvolytic reaction of phenyldisilanes (type 4) under irradiation, we discuss the details of the fluorescence quenching by various alcohols in the subsequent section, on the basis of a whole scheme proposed for photophysical and photochemical processes of **1b**.

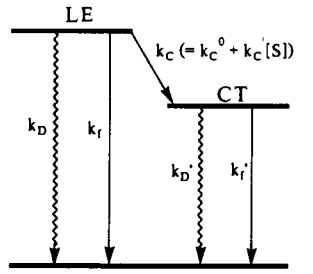

Figure 5. Kinetic profile for the dual fluorescence of **1b** in a mixture of a polar (S) and a nonpolar solvent.

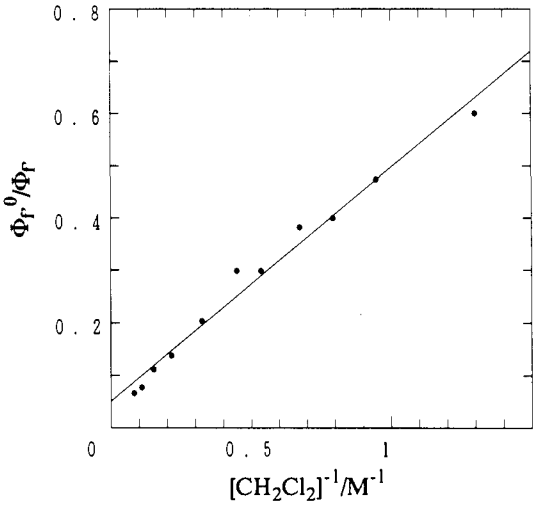

Figure 6. A plot of relative fluorescence quantum yields ($\Phi_f'^0/\Phi_f'$) of **1b** in CH_2Cl_2–hexane mixtures vs $[CH_2Cl_2]^{-1}$.

Photoreactions of 4-(Trifluoromethyl)phenylpentamethyldisilane (1b). Irradiation of **1b** in ethanol–hexane mixtures with a low-pressure Hg arc lamp gave a mixture of the following compounds as volatile products (eq 5); 4-(trifluoromethyl)phenyldimethylsilane (**5**), (trimethylsilyl)[(ethoxydimethyl)silyl]-(trifluoromethyl)cyclohexadienes (**6a** and **6b**), and 4-(trifluoromethyl)phenyl(ethoxydimethyl)silane (**7**). (4-Trifluoromethylphenyl)trimethylsilane, which was expected to be produced via type 3 reaction, was not detected in the reaction mixtures.

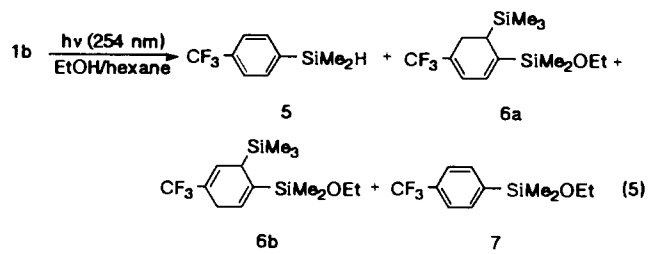

Table III summarizes the results of irradiation of **1b** in various ethanol–hexane mixtures by using a merry-go-round apparatus.

(23) Murov, S. L. *Handbook of Photochemistry*; Marcell Dekker: New York, 1973.

(24) Equation 1 does not mean the unimolecularity of the kinetics but should be taken as an approximate representation of the dependence of k_C on the solvent polarity as a function of power series of $[CH_2Cl_2]$.

(25) Parker, C. A. *Anal. Chem.* **1962**, *34*, 502.

(26) The quenching mechanism of the CT excited state by acetonitrile is not fully understood until now. The CT state may be attacked even by a weak nucleophile such as acetonitrile to be deactivated without cleavage of the Si–Si bond. In this concern, it is interesting to note that carbon–silicon bonds in allylsilane radical cations are assumed to be cleaved by nucleophilic attack by acetonitrile: (a) Ohga, K.; Yoon, U. C.; Mariano, P. S. *J. Org. Chem.* **1984**, *49*, 213. (b) Ohga, K.; Mariano, P. S. *J. Am. Chem. Soc.* **1982**, *104*, 617.

Table III. Chemical and Quantum Yields for the Reaction of **1b** in Ethanol–Hexane Mixtures[a]

[EtOH],[b] M	1b % conv	1b Φ_c	5 % yield	5 Φ_5	6a + 6b % yield	6a + 6b Φ_{6}	7 % yield	7 Φ_7
0.64	97	0.38	0.6	0.0023	72	0.27	5.6	0.021
1.33	68	0.27	0.9	0.0023	74	0.20	5.8	0.015
2.72	57	0.22	2.7	0.0060	70	0.16	7.9	0.018
5.45	49	0.19	7.7	0.014	56	0.11	9.6	0.018
11.0	29	0.11	24	0.027	41	0.046	15	0.017

[a] Irradiation was performed on a 6.94×10^{-3} M solution of **1b** in the mixed solvents with 254-nm light source at 22.0 °C. See Experimental Section for details. [b] Molar concentration of ethanol in hexane.

These products can be easily categorized in the types of reactions shown in Scheme I, while both the chemical and quantum yields depended strongly on the concentration of ethanol in hexane. The compounds **5** and **7** would be formed either by the direct solvolysis (type 4) or via type 1 reaction by accompanying the formation of trimethylethoxysilane (**8**) and trimethylsilane (**9**), respectively.[27,28] These two types of reaction would be differentiated from each other by the experiments using ethanol-d_1 instead of ethanol. Thus, in the presence of ethanol-d_1, type 1 reaction should give a non-deuterated hydrosilane together with an ethoxysilane having deuterium as $SiCH_2D$, while type 4 reaction should give the corresponding deuterosilane and the nondeuterated ethoxysilane. Actually, during the irradiation of **1b** in ethanol-d_1–hexane mixtures, **5** was not detected as undeuterated even in the low concentration of ethanol-d_1.[29] Therefore, in all the present experimental conditions, **5** is concluded to be formed via type 4 reaction involving nucleophilic attack of ethanol at the β-silicon atom. On the other hand, deuterium contents in **7** obtained from the photolysis of **1b** in the presence of ethanol-d_1 varied significantly depending on the concentration of ethanol-d in hexane.[29] The product **7** would be partly formed via type 1 reaction and partly via a direct ethanolysis where nucleophilic attack of alcohol occurs at the α-silicon atom. Compounds **6a** and **6b** are obviously formed by the 1,3-silyl migration from silicon to carbon (type 2).

As shown in Table III, the percent conversion of **1** as well as the quantum yield of the conversion decreased significantly with increasing the concentration of ethanol in hexane. Remarkably the chemical yields and quantum yields of **5** increased, while the combined quantum yields of the 1,3-silyl migration products (**6a** and **6b**) decreased, with increasing the concentration of ethanol. These results suggest that the products **5** and **6** are generated through the different excited states with each other. It would be a reasonable assumption that **5** is produced by the direct solvolysis of the CT excited state, while **6a** and **6b** are produced from the LE state.

The quantum yield for the formation of ethoxysilane **7** did not depend significantly on the concentration of ethanol. As described above, **7** is formed via both type 1 and type 4 reactions and the relative significance of type 4 to type 1 reactions increases with increasing the concentration of ethanol. The apparent independence of the quantum yields on [EtOH] may suggest that the excited states responsible for type 1 and type 4 reactions are the LE and CT states, respectively.

Combining the photochemical processes mentioned above with the photophysical processes shown in Figure 5, the kinetic profile of the photoreactions of **1b** in alcohol–hexane mixtures will be outlined as a whole as shown in Figure 7, where k_5 and k_6 mean the rate constants for the formation of **5** and **6**, respectively, and k_q' is the rate constant for quenching of the CT state by ethanol other than the formation of **5**.[30] On the basis of this scheme, the dependence of the quantum yields on the concentration of the ethanol will be represented by the following equations:

$$\Phi_6 = \frac{k_6}{k_D + k_f + k_6 + k_C^0 + k_C'[\mathrm{EtOH}]} \tag{6}$$

$$\Phi_6^{-1} = \frac{k_D + k_f + k_6 + k_C^0}{k_6} + \frac{k_C'}{k_6}[\mathrm{EtOH}] \tag{7}$$

$$\Phi_5 = \frac{k_C^0 + k_C'[\mathrm{EtOH}]}{k_D + k_f + k_6 + k_C^0 + k_C'[\mathrm{EtOH}]} \times \frac{k_5[\mathrm{EtOH}]}{k_D' + k_f' + (k_5 + k_q')[\mathrm{EtOH}]} \tag{8}$$

if $k_C^0 \ll k_C'[\mathrm{EtOH}]$, then

$$\Phi_5^{-1} = \frac{k_C'(k_5 + k_q')}{k_5 k_C'} + \frac{k_C'(k_D' + k_f') + (k_5 + k_q')(k_D + k_f + k_6 + k_C^0)}{k_5 k_C'}[\mathrm{EtOH}]^{-1} + \frac{(k_D + k_f + k_6 + k_C^0)(k_D' + k_f')}{k_5 k_C'}[\mathrm{EtOH}]^{-2} \tag{9}$$

The validity of these equations was tested by plotting Φ_6^{-1} against [EtOH] and Φ_5^{-1} against $[\mathrm{EtOH}]^{-1}$. Actually, a plot of Φ_6^{-1} vs [EtOH] by using data points obtained from three independent experiments showed a fairly good linear relationship with a slope of 1.71 and an intercept of 2.46 (correlation coefficient, 0.963) (Figure 8).[31] Whereas very complicated dependence of Φ_5 on [EtOH] is derived from eq 8, Φ_5^{-1} is expected to be represented by a second-order function of $[\mathrm{EtOH}]^{-1}$ under the experimental conditions (eq 9). Actually, a plot of Φ_5^{-1} vs $[\mathrm{EtOH}]^{-1}$ fit roughly with eq 9 by assuming appropriate coefficients of the zeroth, first, and second powers of $[\mathrm{EtOH}]^{-1}$ as shown in Figure 9.

(27) Whereas **8** and **9** could not be detected by GLC in this reaction mixture because of the low boiling points, the photolysis of 1-(*p*-trifluoromethylphenyl)-2-hexyltetramethyldisilane (**10**) under similar conditions, the related hexyldimethylethoxysilane and hexyldimethylsilane were obtained in the comparable yields to **5** and **7**. Typically, irradiation of **10** in an ethanol–hexane (3/2 v/v) mixture under a similar condition to that described in the Experimental Section, gave **5**, hexyldimethylethoxysilane, **7**, and hexyldimethylsilane, in the yields of 33, 30, 14, and 16%, respectively.

(28) Mechanistic duality for the formation of arylalkoxysilane during the photolysis of aryldisilanes in the presence of alcohol was actually observed in some cases. Thus, photolysis of 0.15 M solution of **3a** in a methanol-d_1–benzene (1/15 v/v) mixture gave (2-dimethylsilylbenzyl)dimethylmethoxysilane-d_1 (**11**) in 14% yield. ^{2}H NMR analysis showed that the deuterium existed as Si-CH$_2$-*D*, Ar-CH*D*, and Si-*D*, in 81, 7, and 12% relative yields, respectively. On the other hand, similar photolysis of **3a** in methanol-d_1 gave the same methoxysilane in 40% yield, but 87% of the deuterium was incorporated as Si-*D*. It is suggested that **11** is formed mainly via type 4 reaction in methanol, while mainly via type 1 reaction in nonpolar benzene solution. Details will be reported elsewhere.

(29) The photolysis of **1b** (ca. 0.01 M) in ethanol-d_1–hexane (1/4 v/v) and pure ethanol-d_1 gave **5** and **7** whose yields and deuterium contents (in parentheses) were determined by GC-MS spectroscopy as follows: 25.4% of **5** (93.0) and 13.7% of **7** (11.8) in pure ethanol-d_1; 13.6% of **5** (90.6) and 7.88% of **7** (31.7) in ethanol-d_1–hexane (1/4). The deuterium content less than 10% in **5** may be derived from type 1 reaction. Since the small value did not depend seriously on the concentration of ethanol-d_1, the contribution of type 1 reaction for the formation of **5** was ignored in the present discussion about the mechanism. On the other hand, the deuterium content in **7** varied significantly depending on the concentration of ethanol-d_1, suggesting the increasing contribution from type 1 reaction in a less polar solvent. The compound **7** should not be a secondary product from the hydrosilane **5** because an independent experiment showed that **5** was not converted to **7** even under irradiation for a prolonged time.

(30) The rate constant for formation of **7** may be involved in k_q'. The rate constant k_q for the quenching of LE by ethanol was neglected for the sake of simplicity. Primary feature of the dependence of the quantum yields on the concentration of ethanol is reserved even by the inclusion of k_q.

(31) As pointed out by a referee, if the type 1 portion in the product **7** was determined as a function of [EtOH], dependence of the type 1 portion on [EtOH] should match that seen for the formation of **6a** + **6b**. However, the analysis has exceeded the accuracy of the experiment.

Scheme I

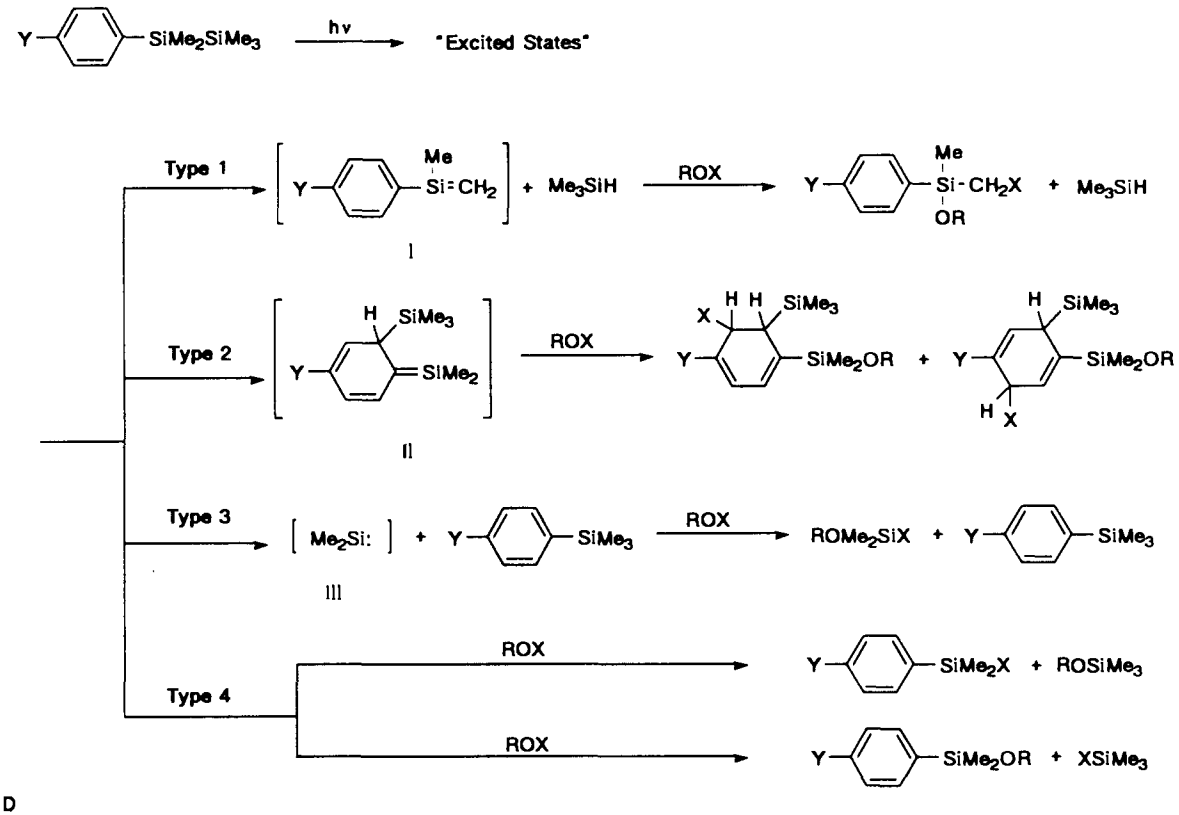

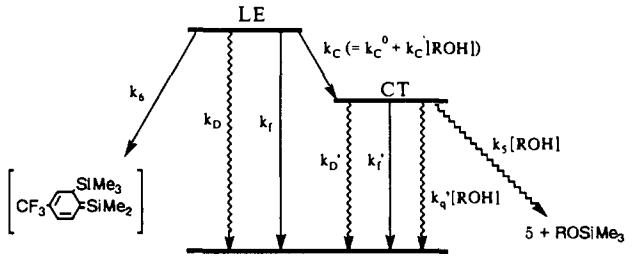

Figure 7. Kinetic profile for photophysical and photochemical processes of **1b** in alcohol–hexane mixtures.

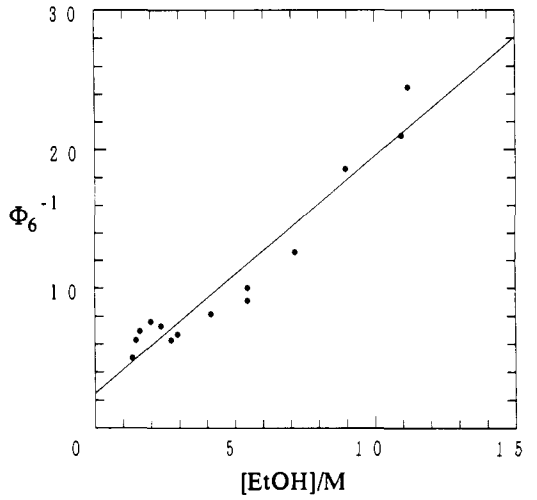

Figure 8. A plot of Φ_6^{-1} vs [EtOH] during irradiation of **1b** in ethanol–hexane mixtures.

Although the fact that quantum yields for the type 2 reaction in the photolysis of phenyl- and naphthylpentamethyldisilanes decrease with increasing solvent polarity has already been recognized by Shizuka et al.,[11d] the superficial conflict with their idea that the photoreaction originates from the intramolecular CT state was avoided by invoking fast intersystem crossing from the CT to $^3(\pi\pi^*)$ state in polar solvents. If type 2 and type 4 reactions occur from the same excited state, either LE or CT, Φ_5/Φ_6 should be proportional to the concentration of ethanol. However, as shown in Figure 10, a plot of Φ_5/Φ_6 vs [EtOH] deviated significantly from proportionality but fit quite well with the following second-order function of [EtOH]: $\Phi_5/\Phi_6 = 5.56 \times 10^{-3}[\mathrm{EtOH}]^2$. The observed relation is in agreement with our model, if $(k_D' + k_f') \gg (k_5 + k_q')[\mathrm{EtOH}]$.

In the above kinetic profile, the CT excited state of **1b** is assumed to be quenched by alcohol and to react partially with the alcohol; the dependence of quantum yields for the CT fluorescence on the concentration of alcohol should be represented by the following equations:

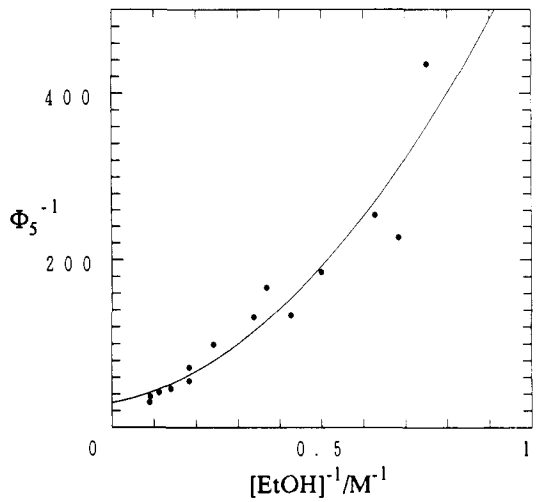

Figure 9. A plot of Φ_5^{-1} vs $[\mathrm{EtOH}]^{-1}$ during irradiation of **1b** in ethanol–hexane mixtures. The solid line is the best fit of the data to eq 9 with the following parameters; 29.46, 96.12, and 4.58×10^2 for the coefficients of zeroth, first, and second powers of $[\mathrm{EtOH}]^{-1}$ in eq 9, respectively.

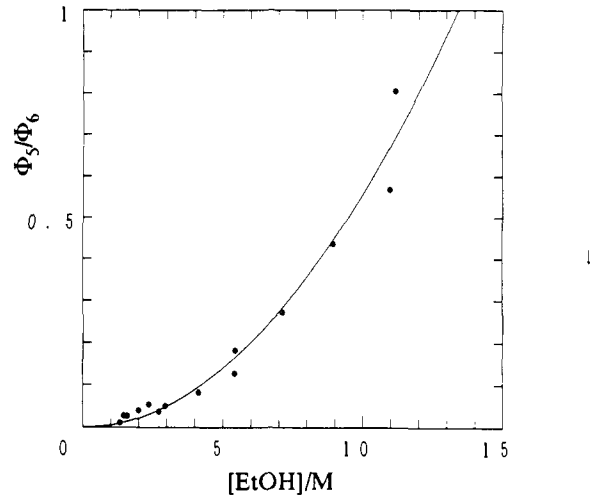

Figure 10. A plot of Φ_5/Φ_6 vs [EtOH] during irradiation of **1b** in ethanol–hexane mixtures.

$$\Phi_f' = \frac{k_C^0 + k_C'[ROH]}{k_D + k_f + k_6 + k_C^0 + k_C'[ROH]} \times \frac{k_f'}{k_D' + k_f' + (k_5 + k_q')[ROH]} \quad (10)$$

if $k_C^0 \ll k_C'[ROH]$, then

$$\frac{\Phi_f'^0}{\Phi_f'}[ROH] = \Phi_f'^0\left\{\frac{(k_D + k_f + k_6 + k_C^0)(k_D' + k_f')}{k_f'k_C'} + \frac{k_C'(k_D' + k_f') + (k_5 + k_q')(k_D + k_f + k_6 + k_C^0)}{k_f'k_C'}[ROH] + \frac{k_C'(k_5 + k_q')}{k_f'k_C'}[ROH]^2\right\}$$

$$= A_f + B_f[ROH] + C_f[ROH]^2 \quad (11)$$

If the fluorescence quenching occurs by collisions between **1b** in excited states and alcohol, the quenching efficiency may depend on the nucleophilicity of alcohols. We have investigated the fluorescence quenching by various alcohols in detail. Plots of $(\Phi_f'^0/\Phi_f')[ROH]$ vs [ROH] are shown in Figure 11. The expected second-order dependence of $(\Phi_f'^0/\Phi_f')[ROH]$ on [ROH] was satisfied quite well. Since the coefficient for $[ROH]^2$, C_f, is parallel to the rate constant for overall quenching by ROH, C_f's for various alcohols are utilized as an index for the relative efficiency of the quenching; $C_f(ROH)/C_f(EtOH)$ were 0.69, 0.52, and 0.08, for R = *i*-Pr, *n*-Bu, and *t*-Bu, respectively. Thus, the order of the quenching efficiency of alcohols for the excited states of **1b** was found as follows: EtOH > *i*-PrOH ≈ *n*-BuOH ≫ *t*-BuOH. The order is compatible to the above mechanism for fluorescence quenching of the CT state by alcohols. Photolysis of **1b** in *t*-BuOH–hexane mixtures gave no products via type 4 reaction but type 2 products in 80–90% yields when [*t*-BuOH] less than 5 M was used; even when [*t*-BuOH] = 8.3 M, only 4% yield of solvolysis products was obtained together with the type 2 products in 85% yield.

Conclusion

Type 2 and type 4 reactions appeared during the photolysis of **1b** in ethanol–hexane mixtures were ascribed unequivocally to the LE and CT excited states, respectively. The mechanistic profile proposed in this paper would be generally adopted to the photoreactions of other aryldisilanes. However, it should be noticed that the nature of the excited states varies significantly

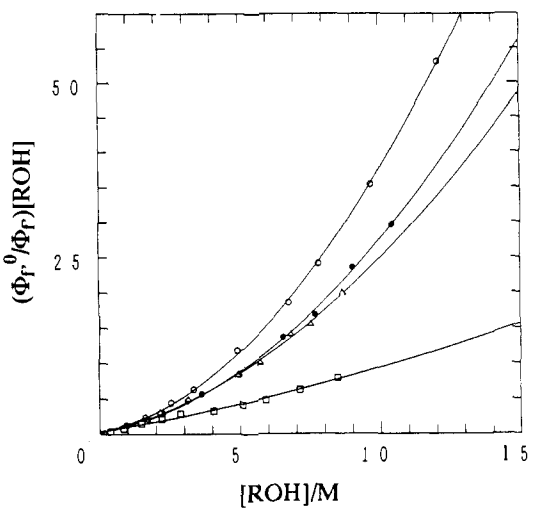

Figure 11. Plots of $(\Phi_f'^0/\Phi_f')[ROH]$ vs [ROH] during irradiation of **1b** in various ROH–hexane mixtures. Parameters, A_f, B_f, and C_f, for the best fit to eq 11 are shown in brackets: EtOH, (○) [0.348, 0.775, 0.294]; *i*-PrOH, (●) [0.329, 0.686, 0.203]; *n*-BuOH, (△) [0.122, 0.939, 0.153]; *t*-BuOH, (□) [0.362, 0.664, 0.0235].

depending on the electronic nature of the aromatic π system. Thus, the relative importance of the solvolytic reaction for CT excited states may increase with increasing the electron-accepting ability of the aromatic π system. During the photolysis of (*p*-cyanophenyl)pentamethyldisilane having a more electron accepting substituent than trifluoromethyl group, type 2 reaction was not observed even in nonpolar solvents. Since the photolysis of *p*-cyanophenyldisilanes gave rather unusual product distribution in the presence of alcohols, the details will be discussed in a forthcoming paper.

Although in the present model, we have reasonably assumed the irreversible formation of the OICT state from the LE state, the LE and the TICT states in (*p*-dimethylamino)benzonitrile are considered to be approaching a thermodynamic equilibrium.[13] In both OICT and TICT systems, the reversibility between the two excited states may depend on the molecular structure, solvent, and so on.

Since the evidence for the existence of type 3 reaction or the formation of free silyl radicals was not obtained during the photolysis of **1b** under various conditions, the excited states responsible for these reactions could not be specified. The present results tell nothing about the detailed mechanism for the formation of the silatriene intermediate (II) from LE; II may be formed either concertedly or via the recombination of an intimiate radical pair consisting of two silyl radicals generated by the homolytic cleavage of the Si–Si bond in the LE excited state, even if the formation of II occurs very rapidly, i.e., within ca. 30 ps, as shown by Shizuka et al.[11c] and Leigh et al.[19]

The observed product ratio, **5**/**7**, does not represent the real regioselectivity of the excited state solvolysis because of the duality of the mechanism for formation of **7**. However, the apparent preference for formation of **5** in a polar solvent system may be acceptable, since the attack of alcohol to the β-Si atom would give rise to a partial negative charge on the α-Si atom, which is stabilized by an electron-withdrawing trifluoromethyl substituent. Solvent dependence of the regioselectivity and the detailed transition-state structure for the alcoholysis of the CT excited state of **1b** remains open.

Experimental Section

General Methods. ^1H, ^{13}C, and ^{29}Si NMR spectra were measured on a Bruker AC-300P (^1H at 300.1 MHz, ^{13}C at 75.5 MHz, and ^{29}Si at 59.6 MHz) and a Bruker AC-600 NMR spectrometers. ^2H NMR spectra were recorded on a JEOL FX-90Q NMR spectrometer. Electron-impact mass spectra was recorded unless otherwise noted at 70 eV on a JEOL

JMS D-300 mass spectrometer. Absorption spectra were measured on a Shimadzu UV-2100 spectrometer.

Solvents. For photochemical and spectroscopic studies, solvents in spectroscopic grade were purchased. EtOH (Kanto), *i*-PrOH (Kanto), and *n*-BuOH (Kanto) were distilled from magnesium before use. *t*-BuOH (Wako) and CH_2Cl_2 (Kanto) was distilled over calcium hydride before use. Hexane (Kanto), pentane (Kanto), and cyclopentane (Merk) were used as such.

Fluorescence Spectra. Fluorescence and the excitation spectra were recorded on a Hitachi M850 fluorescence spectrophotometer. The emission and excitation band-pass was fixed to 5 nm. The fluorescence quantum yields were measured by comparing the fluorescence intensities in reference to that for a hexane solution of naphthalene (1.48×10^{-5} M) at 22–23 °C. All the samples were thoroughly degassed by using freeze–pump–thaw cycles before use.

Fluorescence Lifetimes. The fluorescence lifetimes of substituted phenylpentamethyldisilane were measured in pentane with a Horiba time-resolved spectrofluorometer (NAES-1100). Fluorescence data were collected with a time-correlated single-photon counting apparatus using H_2 flash lamp (NFL-111). The fluorescence life times were determined under irradiation of 250-nm light by fitting the data to a one-component exponential function by minimizing residuals from a convolution of the instrument function.

Quantum Yields of Photoreactions. In a typical experiment, several quartz sample tubes including solutions of **1b** (6.94×10^{-3} M) in various ethanol–hexane mixtures together with a sample tube having a cyclopentane solution of 1-phenyl-2-butene (2.08×10^{-2} M) were irradiated with a low-pressure Hg arc lamp on a Riko rotary photochemical reactor (Model RH400-10W). The light intensity was determined in reference to the progress of the cis–trans isomerization of 1-phenyl-2-butene;[32] the amount of *cis*-1-phenyl-2-butene was corrected for back reaction by method of Lamola.[33] After irradiation for ca. 1.5 h the product yields were determined by means of GLC.

Preparative Photoreaction of 1b (Isolation of 6a and 6b). Typically, a solution of **1b** (44.5 mg, 0.161 mmol) in a mixture of hexane (7 mL) and ethanol (2 mL) in a quartz tube (ϕ 10 mm) was deaerated by argon and then irradiated with a spiral low-pressure mercury arc lamp (125 W) for 2 h. After removal of solvents, preparative GLC gave a 2:1 mixture of **6a** and **6b** as a colorless oil in the combined yield of 42.3% together with small amounts of **5** and **7**. Spectral data for the mixture of **6a** and **6b**: ^{1}H NMR (300.1 MHz, C_6D_6) δ 6.41 (m, 1, **6a**), 6.18 (m, 1, **6b**), 5.84 (m, 1, **6b**), 5.81 (m, 1, **6a**), 3.44 (q, J = 6.9 Hz, 2, **6a** and **6b**), 2.8–2.9 (m, 2, **6b**), 2.56–2.60 (m, 2, **6a**), 2.37 (m, 1, **6b**), 1.94–1.97 (m, 1, **6a**), 1.08 (t, J = 6.9 Hz, 3, **6a** and **6b**), 0.14 (s, 3, **6b**), 0.13 (s, 6, **6a**), 0.10 (s, 3, **6b**), 0.06 (s, 9, **6b**), 0.00 (s, 9, **6a**); MS m/z (rel intensity) 322 (M^+, 2.3), 307 (4), 234 (4), 147 (14), 108 (65), 103 (99), 75 (16), 73 (100), 59 (13), 45 (12); HRMS m/z found 322.1399, calcd for $C_{14}H_{25}OF_3Si_2$ 322.1396.

The compounds **5** and **7** were isolated by preparative GLC from a mixture obtained by similar photolysis of **1b** in ethanol and identified by comparing the spectral data with those of the authentic samples.

4-(Trifluoromethyl)phenylpentamethyldisilane (1b). A mixture of magnesium (0.697 g, 28.9 mmol), chloropentamethyldisilane (1.41 g, 8.48 mmol), and 4-bromo-α,α,α-trifluorotoluene (2.00 g, 8.89 mmol) in THF (10 mL) was stirred for 12 h under reflux. Usual workup gave **1b** in 69.3% yield. **1b**: colorless oil, ^{1}H NMR (300.1 MHz, $CDCl_3$) δ 7.54 (bs, 4), 0.34 (s, 6), 0.04 (s, 9); ^{13}C NMR (75.5 MHz, $CDCl_3$) δ 145.0, 133.9, 130.2 (q, $^2J_{CF}$ = 32.1 Hz), 124.3 (q, $^1J_{CF}$ = 272.0 Hz) 124.1 (q, $^3J_{CF}$ = 3.7 Hz), –2.4, –4.3; ^{29}Si NMR (59.6 MHz, $CDCl_3$) δ –19.2, –20.8; MS m/z (rel intensity) 276 (M^+, 6.6), 261 (12), 203 (50), 184 (82), 73 (100); HRMS m/z found 276.0978, calcd for $C_{12}H_{19}F_3Si_2$ 276.0977; UV (hexane) λ_{max}, nm (ϵ) 239.6 (6820).

6-(Trifluoromethyl)-1-methyl-1-(trimethylsilyl)-1-silaindan (2b). In situ Grignard reaction of 1-bromo-2-(2-bromo-4-(trifluoromethyl)phenyl)ethane (**12**, 0.540 g, 1.63 mmol), magnesium (0.300 g, 12.3 mmol), and 1,1-dichlorotetramethyldisilane (0.460 g, 2.46 mmol) in THF (20 mL) gave **2b** in the yield of 7.3% after purification by preparative gel permeation chromatography (GPC): colorless oil; ^{1}H NMR (300.1 MHz, $CDCl_3$) δ 7.66 (s, 1), 7.46 (d, J = 8.2 Hz, 1), 7.32 (d, J = 8.2 Hz, 1), 3.20 (m, 1), 3.01 (m, 1), 1.24 (m, 1), 1.05 (m, 1), 0.33 (s, 3), 0.09 (s, 9); ^{13}C NMR (75.5 MHz, $CDCl_3$) δ 157.0, 141.4, 128.9 ($^3J_{CF}$ = 3.8 Hz), 127.9 ($^2J_{CF}$ = 31.5 Hz), 124.8 ($^1J_{CF}$ = 272.1 Hz), 125.6 ($^3J_{CF}$ = 3.6 Hz), 125.3, 33.3, 10.5, –2.2, –4.2; ^{29}Si NMR (59.6 MHz, $CDCl_3$) δ –2.9, –19.4; MS m/z (rel intensity) 288 (M^+, 25), 273 (7.4), 215 (32), 196 (100), 73 (95); HRMS m/z found 288.0977, calcd for $C_{13}H_{19}F_3Si_2$ 288.0977; UV (hexane) λ_{max}, nm (ϵ) 234.6 (7630).

6-(Trifluoromethyl)-1,1,2,2-tetramethyl-1,2-disilaindan (3b). In situ Grignard reaction of 2-bromo-4-(trifluoromethyl)benzyl bromide (**13**, 0.558 g, 1.76 mmol), magnesium (0.250 g, 10.3 mmol), and 1,2-dichlorotetramethyldisilane (0.518 g, 2.77 mmol) in THF (10 mL) gave **3b** in 57.4%, which was purified by preparative GPC and then GLC. **3b**: colorless oil; ^{1}H NMR (300.1 MHz, $CDCl_3$) δ 7.67 (s, 1), 7.45 (d, J = 8.2 Hz, 1), 7.27 (d, J = 8.2 Hz, 1), 2.28 (s, 2), 0.32 (s, 6), 0.22 (s, 6); ^{13}C NMR (75.5 MHz, $CDCl_3$) δ 153.5, 143.5, 129.8, 129.7 ($^3J_{CF}$ = 3.6 Hz), 127.1 ($^2J_{CF}$ = 31.7 Hz), 125.7 ($^3J_{CF}$ = 3.6 Hz), 124.7 ($^1J_{CF}$ = 272.2 Hz), 25.8, –3.8, –4.5; ^{29}Si NMR (59.6 MHz, $CDCl_3$) δ –7.4, –15.3; MS m/z (rel intensity) 274 (M^+, 86), 259 (100), 182 (25), 73 (35), 59 (10); HRMS m/z found 274.0821, calcd for $C_{12}H_{17}Si_2F_3$ 274.0821.

(5-(Trifluoromethyl)-2-methylphenyl)pentamethyldisilane (4). In situ Grignard reaction of 3-bromo-4-methylbenzotrifluoride (**14**, 0.54 g, 2.25 mmol), magnesium (0.28 g, 11.6 mmol), and chloropentamethyldisilane (0.380 g, 2.28 mmol) in THF (10 mL) gave **3** in 60.0% yield. The compound **4** was purified by preparative GPC and then GLC. **4**: colorless oil; ^{1}H NMR (300.1 MHz, $CDCl_3$) δ 7.60 (bs, 1), 7.45 (d, J = 8.3 Hz, 1), 7.21 (d, J = 8.3 Hz, 1), 2.43 (s, 3), 0.39 (s, 6), 0.06 (s, 9); ^{13}C NMR (75.5 MHz, $CDCl_3$) δ 147.5, 139.3, 130.8 ($^3J_{CF}$ = 3.6 Hz), 129.5, 127.2 ($^2J_{CF}$ = 31.8 Hz), 125.4 ($^3J_{CF}$ = 3.9 Hz), 124.7 ($^1J_{CF}$ = 271.9 Hz), 23.5, –1.7, –2.8; ^{29}Si NMR (59.6 MHz, $CDCl_3$) δ –18.7, –20.8; MS m/z (rel intensity) 290 (M^+, 6.9), 275 (26), 217 (77), 198 (100), 73 (73); HRMS m/z found 290.1136, calcd for $C_{13}H_{21}Si_2F_3$ 290.1134; UV (hexane) λ_{max}, nm (ϵ) 236.5 (8270).

1-(4-(Trifluoromethyl)phenyl)-2-hexyltetramethyldisilane (9). To a solution of 4-bromo-α,α,α-trifluorotoluene (1.296 g, 5.76 mmol) in dry diethyl ether (10 mL) was added slowly a hexane solution of *n*-butyllithium (1.66 M, 3.8 mL) at –90 °C. After stirring for 4 h, 1-chloro-2-hexyltetramethyldisilane (1.10 g, 4.64 mmol) was added to the reaction mixture and then stirred for 12 h. Silica gel column chromatography (hexane) and then Kugelrohr distillation gave **9** in 73.3% yield (1.18 g, 3.40 mmol). **9**: colorless oil; ^{1}H NMR (300.1 MHz, $CDCl_3$) δ 7.57 (bs, 4), 1.25 (bs, 8), 0.87 (m, 3), 0.59 (m, 2), 0.38 (s, 6), 0.05 (s, 6); ^{13}C NMR (75.5 MHz, $CDCl_3$) δ 145.4, 133.9, 130.3 (q, $^2J_{CF}$ = 32.2 Hz), 124.4 (q, $^1J_{CF}$ = 272.1 Hz), 124.2 (q, $^3J_{CF}$ = 3.7 Hz), 33.3, 31.6, 24.5, 22.6, 14.7, 14.1, –3.8, –4.2; ^{29}Si NMR (59.6 MHz, $CDCl_3$) δ –17.3, –20.8; MS m/z (rel intensity) 346 (M^+, 2.8), 203 (21), 185 (15), 184 (89), 143 (30), 87 (13), 77 (15), 73 (42), 59 (100); HRMS m/z found 346.1766, calcd for $C_{17}H_{29}F_3Si_2$ 346.1760.

1-Bromo-2-(2-bromo-4-(trifluoromethyl)phenyl)ethane (12). Bromine (8.00 g, 50.0 mmol) was added to a suspension of 1-(4-(trifluoromethyl)phenyl)-2-bromoethane[34] (4.9 g, 19.4 mmol) and iron (4.00 g, 71.6 mmol) in dichloromethane (20 mL). After refluxing for 24 h, the reaction mixture was poured into a saturated aqueous solution of $NaHSO_3$ and extracted with hexane. Kugelrohr distillation gave **12** in 65.2% yield. **12**: colorless oil; ^{1}H NMR (300.1 MHz, $CDCl_3$) δ 7.80 (bs, 1), 7.52 (d, J = 8.0 Hz, 1), 7.38 (d, J = 8.0 Hz, 1), 3.59 (t, J = 7.3, 2), 3.33 (t, J = 7.3 Hz, 2); ^{13}C NMR (75.5 MHz, $CDCl_3$) δ 142.0, 131.5, 131.0 (q, $^2J_{CF}$ = 33.1 Hz), 130.0 (q, $^3J_{CF}$ = 3.8 Hz), 124.4, 124.4 (q, $^3J_{CF}$ = 3.9 Hz), 123.1 (q, $^1J_{CF}$ = 272.4 Hz), 39.2, 30.2; MS m/z (rel intensity) 334 (25), 332 (45), 330 (26), 254 (10), 253 (98), 252 (17), 251 (100), 239 (84), 237 (88), 172 (74), 151 (72), 102 (30); HRMS m/z found 329.8864, calcd for $C_9H_7{}^{79}Br_2F_3$ 329.8866.

2-Bromo-4-(trifluoromethyl)benzyl Bromide (13). Bromine (10 g, 62.6 mmol) was added to a suspension (20 mL) of 4-(trifluoromethyl)benzylbromide (4.9 g, 20.5 mmol) and iron (20 g, 0.358 mol) in dichloromethane. After refluxing for 24 h, the reaction mixture was poured into a saturated aqueous solution of $NaHSO_3$ and extracted with hexane. Kugelrohr distillation gave **13** in the yield of 37%. **13**: colorless oil; ^{1}H NMR (300.1 MHz, $CDCl_3$) δ 7.82 (bs, 1), 7.54 (m, 2), 4.58 (s, 2); ^{13}C NMR (75.5 MHz, $CDCl_3$) δ 141.0, 132.0 (q, J = 33.4 Hz), 131.5, 130.3 (q, $^3J_{CF}$ = 3.7 Hz), 124.8 (q, $^3J_{CF}$ = 3.9 Hz), 124.5, 122.8 (q, $^1J_{CF}$ = 273.0 Hz), 31.8; MS (EI, 70 eV) m/z (rel intensity) 320 (7), 318 (15), 316 (8), 240 (9), 239 (96), 238 (10), 237 (100), 158 (39), 157 (13), 138 (13), 107 (11), 89 (14); HRMS m/z found 315.8713, calcd for $C_8H_5{}^{79}Br_2F_3$ 315.8710.

3-Bromo-4-methylbenzotrifluoride (14). Bromine (5.00 g, 31.3 mmol) was added to a suspension of 4-(trifluoromethyl)toluene (2.30 g, 14.4 mmol) and iron (2.00 g, 35.8 mol) in dichloromethane (10 mL). After

(32) Morrison, H.; Peiffer, R. *J. Am. Chem. Soc.* **1968**, *90*, 3428.
(33) Lamola, A. A.; Hammond, G. S. *J. Phys. Chem.* **1965**, *43*, 2129.
(34) Dive, V.; Yiotakis, A.; Nicolaou, A.; Toma, F. *Eur. J. Biochem.* **1990**, *191*, 685.
(35) Buell, G. R.; Corriu, R.; Guerin, C.; Spialter, L. *J. Am. Chem. Soc.* **1970**, *92*, 7424.

stirring at room temperature for 24 h, the reaction mixture was poured into a saturated aqueous solution of $NaHSO_3$ and then extracted with hexane. Kugelrohr distillation gave **14** in 93.1% yield. **14**: colorless oil; ^{1}H NMR (300.1 MHz, $CDCl_3$) δ 7.78 (s, 1), 7.44 (d, J = 7.8 Hz, 1), 7.31 (d, J = 7.8 Hz, 1), 2.43 (s, 3); ^{13}C NMR (75.5 MHz, $CDCl_3$) δ 142.2, 131.0, 129.7 (q, $^2J_{CF}$ = 32.8 Hz), 129.2 (q, $^3J_{CF}$ = 3.9 Hz), 124.9, 124.0 (q, $^3J_{CF}$ = 3.9 Hz), 123.3 (q, $^1J_{CF}$ = 271.9 Hz), 22.9; MS (EI, 70 eV) m/z (rel intensity) 240 (50), 238 (55), 159 (100), 158 (25), 109 (31); HRMS m/z found 237.9606, calcd for $C_8H_6{}^{79}BrF_3$ 237.9605.

(4-(Trifluoromethyl)phenyl)dimethylsilane (5). A mixture of 4-bromo-α,α,α-trifluorotoluene (2.91 g, 12.9 mmol) and dimethylchlorosilane (2.91 g, 30.7 mmol) in dry THF (5 mL) was added to magnesium (0.700 g, 28.9 mmol) in THF. The reaction mixture was refluxed for 12 h. Usual workup gave **5** (2.00 g 9.79 mmol, 75.9%). **5**: colorless oil; ^{1}H NMR (300.1 MHz, $CDCl_3$) δ 7.67 (d, J = 8.1 Hz, 2), 7.61 (d, J = 8.1 Hz, 2) 4.48 (sep, J = 3.8 Hz, 1), 0.39 (d, J = 3.8 Hz, 6); ^{13}C NMR (75.5 MHz, $CDCl_3$) δ 142.5, 134.3, 131.2 (q, $^2J_{CF}$ = 32.2 Hz), 124.4 (q, $^3J_{CF}$ = 3.9 Hz), 124.2 (q, $^1J_{CF}$ = 272.1 Hz), -4.1; ^{29}Si NMR (59.6 MHz, $CDCl_3$) δ -16.2; MS m/z (rel intensity) 203 (M^+ - 1, 26.5), 189 (100), 173 (12.7), 127 (40.5), 108 (70.9), 81 (11.5), 77 (48.1), 58 (10.3). Anal. Calcd for $C_9H_{11}F_3Si$: C, 52.92; H, 5.43. Found: C, 52.65; H, 5.46.

(4-(Trifluoromethyl)phenyl)(ethoxydimethyl)silane (7). A mixture of 4-bromo-α,α,α-trifluorotoluene (2.57 g, 11.4 mmol) and diethoxydimethylsilane (2.58 g, 17.4 mmol) in dry THF (5 mL) was added to 0.700 g (28.9 mmol) of magnesium in THF. The reaction mixture was refluxed for 12 h. Filtration after exchange of the solvent to hexane and then usual workup gave **7** (1.63 g, 6.56 mmol, 57.5%). **7**: colorless oil; ^{1}H NMR (300.1 MHz, $CDCl_3$) δ 7.70 (d, J = 8.0 Hz, 2), 7.61 (d, J = 8.0 Hz, 2), 3.69 (q, J = 7.0 Hz 2), 1.20 (t, J = 7.0 Hz, 3), 0.40 (s, 6); ^{13}C NMR (75.5 MHz, $CDCl_3$) δ 143.0, 133.6, 131.4 (q, $^2J_{CF}$ = 32.1 Hz), 124.2 (q, $^3J_{CF}$ = 3.7 Hz), 122.2 (q, $^1J_{CF}$ = 272.1 Hz), 58.7, 18.2, -2.0; ^{29}Si NMR (59.6 MHz, $CDCl_3$) δ 6.8; MS m/z (rel intensity) 233 (100), 205 (35.2), 203 (20.8), 189 (52.9), 153 (15.9). Anal. Calcd for $C_{11}H_{15}OF_3Si$: C, 53.21; H, 6.09. Found: C, 52.92; H, 6.10.

Ethoxyhexyldimethylsilane.[35] Diethoxydimethylsilane (4.0 g, 27 mmol) in THF (20 mL) was added to hexylmagnesium chloride prepared from 1-chlorohexane (5.0 g, 41 mmol) and magnesium (1.1 g, 45 mmol) in THF (15 mL). Refluxing the mixture for 12 h and then usual workup gave the title compound as a colorless oil in 30% yield: ^{1}H NMR (300.1 MHz, $CDCl_3$) δ 3.6 (q, J = 7.0 Hz, 2), 1.26 (m, 8), 1.16 (t, J = 7.0 Hz, 3), 0.86 (m, 3), 0.57 (m, 2), 0.066 (s, 6); ^{13}C NMR (75.5 MHz, $CDCl_3$) δ 58.2, 33.1, 31.6, 23.1, 22.6, 18.5, 16.4, 14.1, -2.1; ^{29}Si NMR (59.6 MHz, $CDCl_3$) δ 17.3.

(4-Cyanophenyl)pentamethyldisilane. To a solution of 4-bromobenzonitrile (1.98 g, 10.9 mmol) in dry THF (30 mL) was added a *n*-pentane solution of *tert*-butyllithium (1.62 M, 8 mL) at -100 °C and then stirred for 4 h. After addition of chloropentamethyldisilane (1.87 g, 11.2 mmol), the reaction mixture was stirred further for 12 h. Usual workup and then Kugelrohr distillation gave (4-cyanophenyl)pentamethyldisilane in 58.0% yield (1.53 g, 6.5 mmol): ^{1}H NMR (300.1 MHz, $CDCl_3$) δ 7.57 (d, J = 8.1 Hz, 2), 7.51 (d, J = 8.1 Hz, 2), 0.33 (s, 6), 0.02 (s, 9); ^{13}C NMR (75.5 MHz, $CDCl_3$) δ 147.2, 134.0, 130.8, 119.1, 111.7, -2.5, -4.5; ^{29}Si NMR (59.6 MHz, $CDCl_3$) δ -19.0, -20.0; MS m/z (rel intensity) 233 (29), 160 (23), 73 (100), 45 (18), 43 (20); HRMS m/z found 233.1046, calcd for $C_{12}H_{19}NSi_2$ 233.1056; UV (hexane) λ_{max}, nm (ϵ) 228.5 (9330), 257.4, (11 480).

Acknowledgment. This research was supported in part by Ministry of Education, Science, and Culture (Grand-in Aids for Specially Promoted Research No. 02102004).